

# A Primary Xenograft Model of Small-Cell Lung Cancer Reveals Irreversible Changes in Gene Expression Imposed by Culture *In vitro*

Vincent C. Daniel,<sup>1</sup> Luigi Marchionni,<sup>2</sup> Jared S. Hierman,<sup>2</sup> Jonathan T. Rhodes,<sup>2</sup> Wendy L. Devereux,<sup>2</sup> Charles M. Rudin,<sup>2</sup> Rex Yung,<sup>2</sup> Giovanni Parmigiani,<sup>2,3,4</sup> Marion Dorsch,<sup>5</sup> Craig D. Peacock,<sup>2</sup> and D. Neil Watkins<sup>2,6</sup>

Departments of <sup>1</sup>Surgery, <sup>2</sup>Oncology, <sup>3</sup>Biology, and <sup>4</sup>Pathology, Sidney Kimmel Comprehensive Cancer Center, Johns Hopkins University School of Medicine, Baltimore, Maryland; <sup>5</sup>Novartis Institutes of Biomedical Research, Cambridge, Massachusetts; and <sup>6</sup>Monash Institute of Medical Research, Monash University, Clayton, Victoria, Australia

## Abstract

**Traditional approaches to the preclinical investigation of cancer therapies rely on the use of established cell lines maintained in serum-based growth media. This is particularly true of small-cell lung cancer (SCLC), where surgically resected tissue is rarely available. Recent attention has focused on the need for better models that preserve the integrity of cancer stem cell populations, as well as three-dimensional tumor-stromal interactions. Here we describe a primary xenograft model of SCLC in which endobronchial tumor specimens obtained from chemo-naïve patients are serially propagated *in vivo* in immunodeficient mice. In parallel, cell lines grown in conventional tissue culture conditions were derived from each xenograft line, passaged for 6 months, and then reimplanted to generate secondary xenografts. Using the Affymetrix platform, we analyzed gene expression in primary xenograft, xenograft-derived cell line, and secondary xenograft, and compared these data to similar analyses of unrelated primary SCLC samples and laboratory models. When compared with normal lung, primary tumors, xenografts, and cell lines displayed a gene expression signature specific for SCLC. Comparison of gene expression within the xenograft model identified a group of tumor-specific genes expressed in primary SCLC and xenografts that was lost during the transition to tissue culture and that was not regained when the tumors were reestablished as secondary xenografts. Such changes in gene expression may be a common feature of many cancer cell culture systems, with functional implications for the use of such models for preclinical drug development. [Cancer Res 2009;69(8):3364–73]**

## Introduction

Lung cancer is the commonest cause of cancer death in the United States (1). Of these, ~15% to 20% of cases are small-cell lung cancer (SCLC), a highly aggressive, primitive neuroendocrine tumor that is often widely metastatic at the time of diagnosis. Most cases of SCLC are initially sensitive to cytotoxic chemotherapy, despite the fact that most of these tumors lack both p53 and pRB

and manifest overexpression of BCL2 (2). Regimens based on *cis*-platinum, usually in combination with etoposide, result in robust and often dramatic clinical responses in SCLC patients (3). Despite the effectiveness of this drug combination, the overwhelming majority of SCLC patients succumb to a chemoresistant recurrence within 2 years of diagnosis (3). Neither the use of novel chemotherapeutics nor the introduction of dose intensification regimens has improved survival, which has remained essentially unchanged for the last 30 years (3). The clinical imperative in SCLC is the discovery of novel strategies to prevent disease recurrence.

For three decades, the mainstay of preclinical cancer therapeutic research has been the use of human cancer cells lines cultured *in vitro* and of xenografts derived from these cell lines grown *in vivo* in immunodeficient mice. Neither of these models consistently predict efficacy in clinical trials, resulting in two major barriers to the successful translation of new cancer therapeutics. First, resources are expended on drug development based on these models that ultimately fail in clinical trials. Second, many potentially useful therapies that might be beneficial in humans are discarded because they fail to show efficacy in conventional cell culture and xenograft models. Emerging evidence suggests that the process of establishing conventional cell lines from human cancers results in distinct and irreversible loss of important biological properties, which include (a) gain or loss of gene amplification (4, 5), (b) the ability to migrate and metastasize (6), (c) the maintenance of a distinct stem cell population (6), and (d) the preservation of dependency on embryonic signaling pathways (7, 8). In all cases, these properties are not restored when these conventional cell lines are grown as heterotopic or orthotopic xenografts.

Preclinical modeling of SCLC chemotherapy presents challenges in addition to those outlined above. Because SCLC is usually diagnosed by endobronchial biopsy or fine-needle aspiration cytology, substantial quantities of fresh or frozen tissues are typically lacking in most tumor banks. For this reason, most SCLC researches rely on conventional cell lines, which are often chemoresistant because they were derived from patients who had received cytotoxic chemotherapy (9). In addition, all of these cell lines suffer from the experimental limitations outlined above and lack the three-dimensional tumor-stromal interactions, which seem to significantly affect the response of these cells to chemotherapy (10). As part of our ongoing efforts to develop better models for the study of SCLC, we generated and characterized a series of primary xenograft models derived from chemo-naïve patients to more accurately model this disease. In our first description of this primary xenograft model, we showed that differential expression of BCL2 *in vivo* was correlated with growth responses to the BCL2 inhibitor ABT-737 (11). Here, we describe a detailed gene

**Note:** Supplementary data for this article are available at Cancer Research Online (<http://cancerres.aacrjournals.org/>).

V.C. Daniel, L. Marchionni, and J.S. Hierman contributed equally to this work.

**Requests for reprints:** D. Neil Watkins, Monash Institute of Medical Research, Monash Medical Center, 246 Clayton Road, Clayton, Vic 3168, Australia. Phone: 61-3-9594-7165; Fax: 61-3-9594-7167; E-mail: [neil.watkins@med.monash.edu.au](mailto:neil.watkins@med.monash.edu.au) or Craig D. Peacock, Sidney Kimmel Comprehensive Cancer Center, Johns Hopkins University School of Medicine, Room 546, 1550 Orleans Street, Baltimore, MD 21231. E-mail: [cpeacock3@jhmi.edu](mailto:cpeacock3@jhmi.edu).

©2009 American Association for Cancer Research.

doi:10.1158/0008-5472.CAN-08-4210

expression analysis of this model that reveals how gene expression is irreversibly altered during the process of establishing conventional cell culture, and how maintenance of SCLC xenografts passaged exclusively *in vivo* can retain features of the primary tumor of direct relevance to preclinical drug testing.

## Materials and Methods

### Generation and maintenance of primary xenografts and cell lines.

Over an 18-mo period, discarded tissues from three chemo-naive SCLC patients undergoing therapeutic bronchoscopy for acute bronchial obstruction were obtained fresh and transported to the laboratory in 1× PBS at 4°C. All samples were anonymized and obtained in accordance with the Johns Hopkins University Institutional Review Board. Due to the small amount of material available, the entire sample was used to generate a xenograft. Under aseptic conditions, tumor samples were finely minced with razor blades, vigorously triturated in 1× PBS, passed through a 60- $\mu$ m filter, centrifuged, and then resuspended in 500  $\mu$ L of Matrigel (BD Biosciences) at 4°C. Cells were then injected s.c. in the flanks of five nonobese diabetic/severe combined immunodeficient mice that were monitored for tumor growth. When the P0 tumors reached 1 cm in diameter, the mouse was sacrificed and the tumor divided into sections for snap freezing, frozen tissue sectioning, formalin fixation, conventional cell culture, or serial passage. All animal studies were done in accordance with protocols approved by the Johns Hopkins University Animal Care and Use Committee.

Serial passage *in vivo* was done by disaggregating the tumor as described above. Aliquots of cells were then injected into the flanks of athymic nude mice in Matrigel or cryopreserved in 90% RPMI (Invitrogen)/10% DMSO (Sigma). Conventional cell lines were established by seeding an aliquot of disaggregated cells in culture with advanced RPMI (Invitrogen)/1% bovine calf serum (Invitrogen). Cell lines were passaged and cryopreserved in standard fashion for SCLC cultures. Publicly available SCLC cell lines were obtained from American Type Culture Collection (ATCC) and cultured in advanced RPMI (Invitrogen)/1% bovine calf serum. Xenografts derived from these conventional cell lines were grown in the flanks of nude mice as described above. Orthotopic xenografts were generated by dorsoscapular, transcutaneous injection of cells suspended in Matrigel into the right lung of nude mice, essentially as described (12).

**Assessment of SCLC phenotype.** At each passage *in vivo* and at every 3 mo *in vitro*, cell suspensions were immunophenotyped by fluorescence-activated cell sorting (FACS) analysis (FACSCalibur, BD Biosciences) with antibodies to human CD56 (BD Biosciences). Genomic DNA was purified using DNAzol (Invitrogen). Total RNA was purified using RNAzol (Invitrogen), followed by a secondary purification using the RNEasy system (Qiagen). Standard Affymetrix expression microarray protocols were used for all array studies.

**Gene expression annotation and preprocessing.** Gene expression analysis from our xenograft samples was assumed to be human specific based on (a) quantitative reverse transcription-PCR (RT-PCR) analysis showing that mouse mRNA contributed between 1/8 and 1/16 of the total mRNA (data not shown), and (b) probe sets developed by Affymetrix that are highly specific for each species.<sup>7</sup> We complemented our gene expression experiments with additional data sets retrieved from the National Center for Biotechnology Information (NCBI) Gene Expression Omnibus (GEO) database (13). Gene annotation for all the platforms considered was obtained from R-Bioconductor metadata packages (14). For a complete description of platforms and data sets, see Supplementary Table S1. Raw gene expression intensities for all samples were normalized at the probe level using the RMA algorithm as described by Irizarry and colleagues (15). To compare gene expression across different Affymetrix platforms, we first used Entrez Gene identifiers as cross-referencing keys, and then matched all the individual probes at the sequence level to those contained in the

hgu133a platform to control laboratory and batch effects using the “barcode” RMA preprocessing algorithm described by Zilliox and Irizarry (16). Standardization across DNA chips was attained by quantile normalization (17). Details are reported in Supplementary Figs. S17 and S18.

**Differential gene expression analysis.** In all data sets considered in the present study, differential gene expression was investigated using functions and methods implemented in the R/Bioconductor (14, 18) package limma

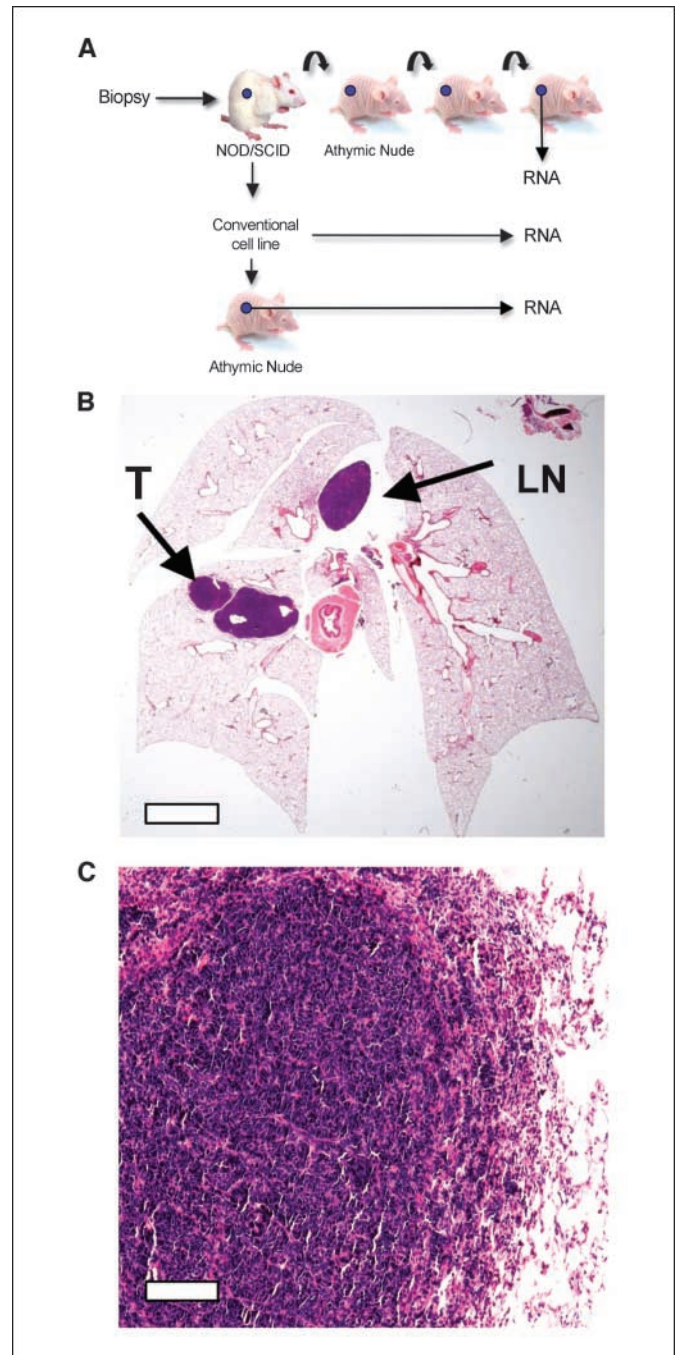


**Figure 1.** Generation and characterization of the SCLC primary xenograft model. *A*, outline of the experimental approach from primary sample, xenograft, cell line, and secondary xenograft from the derived cell line. *NOD/SCID*, nonobese diabetic/severe combined immunodeficient. *B*, H&E-stained section of mouse lungs following orthotopic injection of the LX22 xenograft. The “primary” tumor (*T*) and metastasis in mediastinal lymph node (*LN*) are highlighted. Bar, 1 mm. *C*, H&E-stained section of the intrapulmonary tumor shown in *B*. Bar, 20  $\mu$ m.

<sup>7</sup> [http://www.affymetrix.com/support/technical/comparison\\_spreadsheets.affx](http://www.affymetrix.com/support/technical/comparison_spreadsheets.affx)

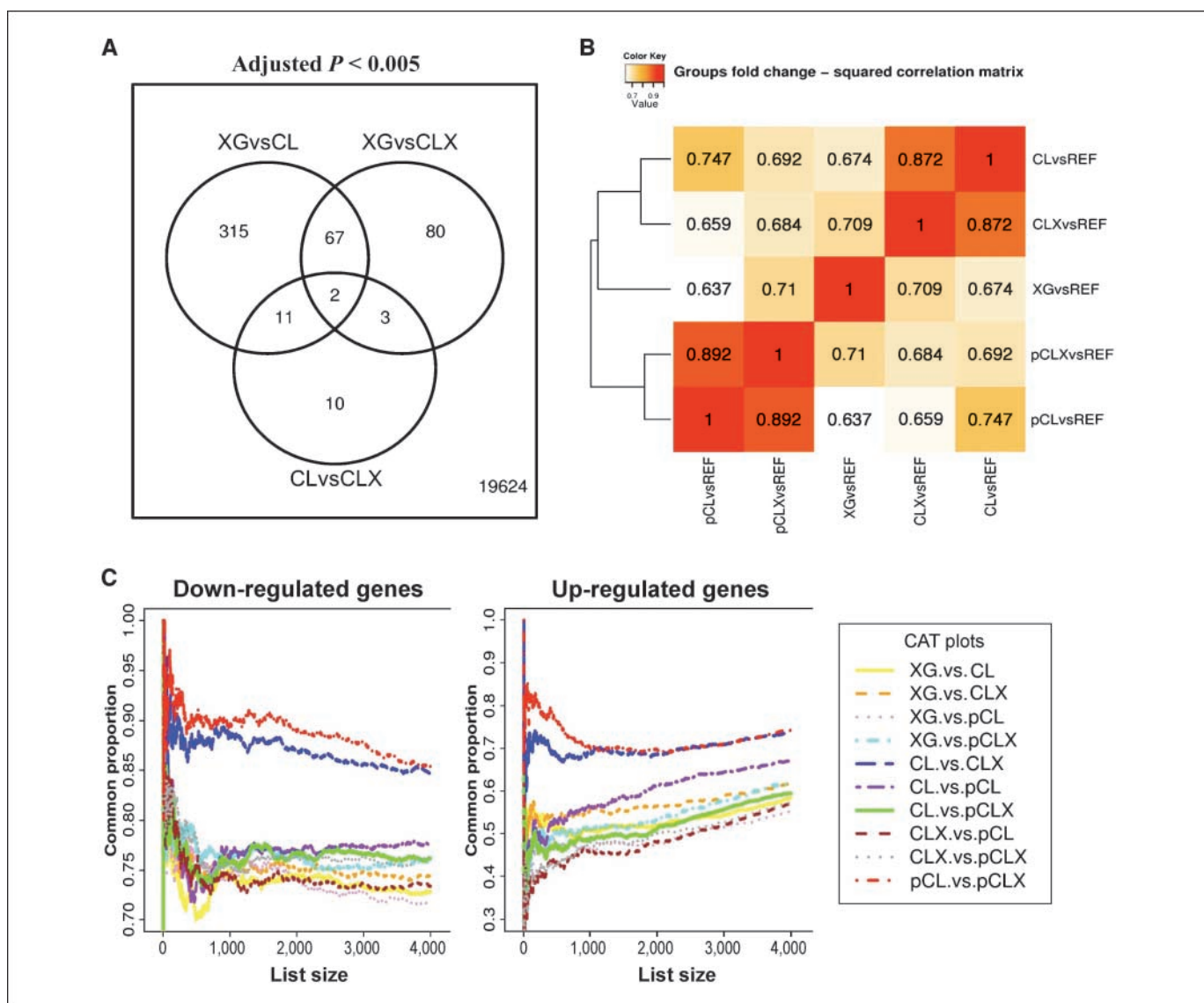


**Figure 2.** Differential expression analysis in the primary xenograft model. **A**, Venn diagram showing the number of differentially expressed genes (adjusted  $P < 0.005$ ) in direct comparisons among primary xenografts (XG), the matched cell lines (CL), and the xenografts obtained from these cell lines (CLX). Only 26 genes were differentially expressed between CL and CLX (CLvsCLX), 152 between XG and CLX (XGvsCLX), and 395 between XG and CL (XGvsCL). **B**, hierarchical clustering of pairwise squared correlations between distinct groups of samples. Matched triplets of samples are denoted as XG, CL, and CLX, whereas pairs of independent samples from established cell lines and from the public domain (CL and CLX) are denoted by the prefix "p." All correlations were computed between mean fold changes of each sample group compared with the universal reference RNA (Stratogene). Comparisons involving CL and CLX groups (CLvsREF, CLXvsREF, pCLvsREF, and pCLXvsREF) proved to be more correlated than any other comparison involving the primary xenografts group (XGvsREF). **C**, CAT plots for all pairwise comparisons among triplets and pairs of samples. The notation used is the same as in **A** and **B**. Genes were ranked by the mean fold change of each sample group compared with the universal reference RNA. On the left is shown the correspondence for the most down-regulated genes (4,000), and on right for the most up-regulated genes (400). The red and the blue lines on the top of the CAT plot represent the comparisons between CL and CLX for matched triplets and pairs of samples and show the highest correspondence. For the up-regulated genes, the purple line represents the comparison between cell lines derived from our xenografts (CL) and cell lines from the public domain (pCL). This comparison shows more similarity than when XG are compared with CL.

(19). Briefly, a fixed effects linear model was fit for each individual feature to estimate expression differences between groups of samples to be compared. When technical replicates or matched samples from the same individual were available, replicates were used as blocks and the average correlation within the blocks was estimated and used in the model (20). An empirical Bayes approach was applied to moderate SEs of normalized logarithmic fold change ( $M$  values; ref. 19). Finally, for each analyzed feature, moderated  $t$  statistics, log odds ratios of differential expression ( $B$  statistics), raw and adjusted  $P$  values (FDR control by the Benjamini and Hochberg method;

ref. 21) were obtained. Details are reported in Supplementary Data. Raw expression data and the MIAME required information are currently available online<sup>8</sup> and will be permanently hosted in the GEO database on publication.

**Analysis of functional annotation.** To capture biological processes relevant in the investigated sample groups, we performed analysis of functional annotation. Functional gene sets, in the form of lists of genes sharing specific biological properties, were obtained from the Gene Ontology (GO) database (22–24), KEGG pathway database (25), and Molecular Signature Database (MsigDb)<sup>9</sup> (26). The analysis of functional

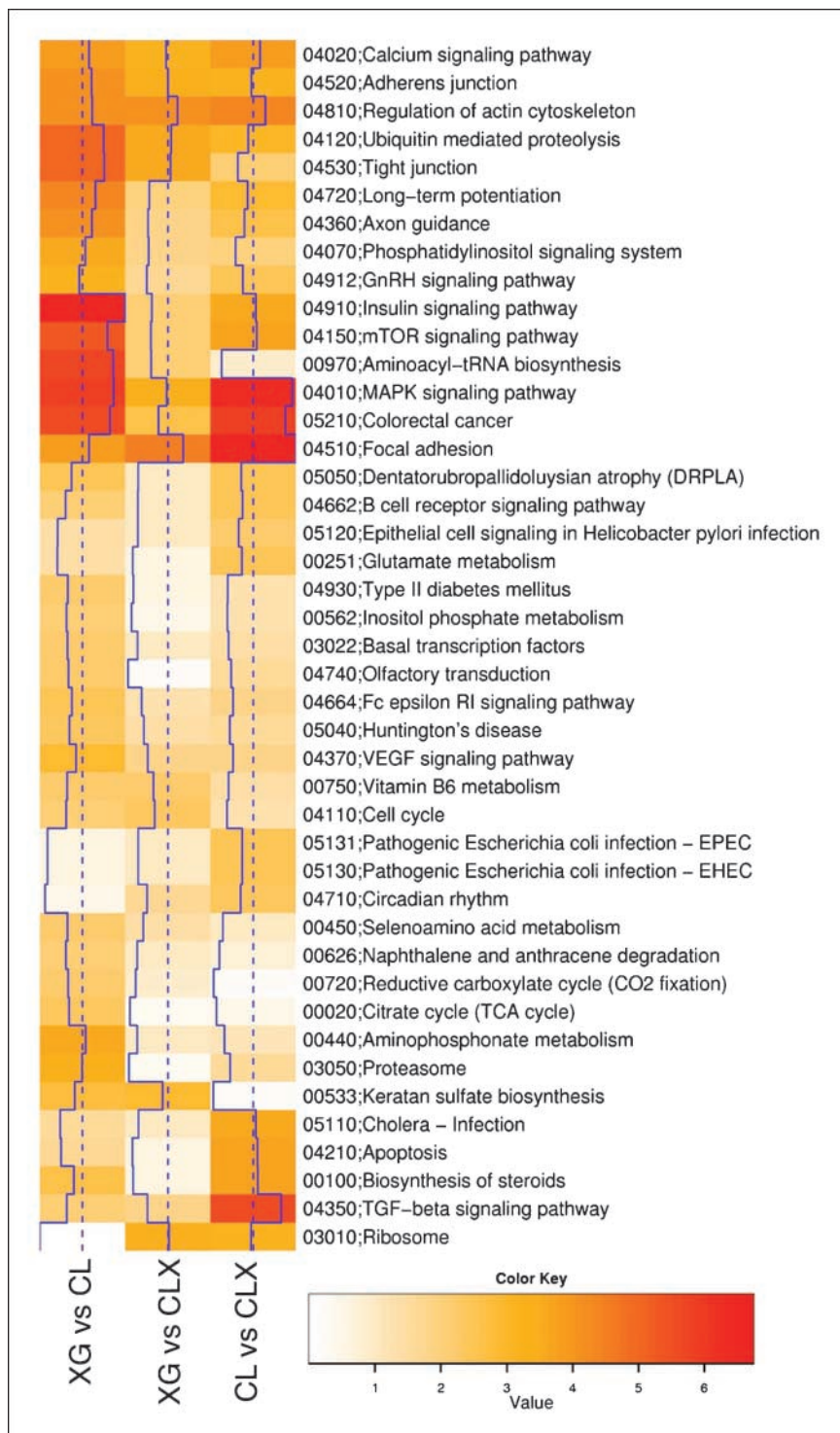
<sup>8</sup> <http://astor.som.jhmi.edu/~marchion/sclc.html>

<sup>9</sup> <http://www.broad.mit.edu/gsea/msigdb/msigdb/index.html>

annotation was done by one-sided Wilcoxon test after ranking the genes by their absolute moderated  $t$  statistics. Multiple testing correction was done separately for each functional scope (GO, KEGG, and MsigDb) by the Benjamini and Hochberg method (21). Mappings between individual probes on the array to the various functional themes were based on NCBI Entrez Gene identifiers obtained from the R-Bioconductor metadata packages. Overall, this approach is analogous to Gene Set Enrichment Analysis (GSEA)-like procedures (26, 27). Details are reported in Supplementary Data.

**Relationships among different sample groups.** To compare gene expression data among distinct sample groups, we compared the lists of differentially expressed genes obtained from the linear model analysis; we computed the squared correlation between normalized gene expression measurements and log<sub>2</sub> fold-changes ( $M$  values) across samples; and we used the “correspondence-at-the-top” plot (CAT plot) technique (28). This latter method is specifically designed to assess the agreement and similarity between microarray experiments, where it is expected that only a small fraction of genes would be differentially expressed across the large total

**Figure 3.** Analysis of functional annotation. Heat map showing analysis of functional annotation results for KEGG pathways. Color-coded values correspond to absolute values of base 10 logarithms of raw  $P$  values from the Wilcoxon rank-sum test. Vertical blue lines show the same data as a histogram value for each color intensity. All pathways shown proved to be enriched in at least one comparison (adjusted  $P < 0.05$ ). Rows were clustered using Euclidian distance and the average clustering method; columns were not reordered. Several pathways showed significant results changes in all comparisons, although different sets of genes proved to be responsible for the enrichment, whereas a number of pathways (i.e., Keratan sulfate biosynthesis) proved to be enriched in a subset of the contrasts considered (see Supplementary Tables A–C for genes involved and analysis of additional functional scopes, including GO).



number of analyzed genes. Principal coordinates analysis and multidimensional scaling were done using 1 – correlation as a measure of distance. Details are reported in Supplementary Data.

## Results

**Characterization of the primary SCLC xenograft model.** An overview of the experimental model is shown in Fig. 1A. With serial passage *in vivo*, all three primary xenograft lines (LX22, LX33, and LX36) maintained a typical histopathologic appearance (ref. 11 and data not shown). Cell lines derived from each of these xenografts grew as loose aggregates or spheroids typical of SCLC cell lines (ref. 9; data not shown). Immunohistochemical and FACS analyses of freshly isolated cells from each xenograft showed strong expression of human CD56, a marker of neural differentiation in >95% of the cells (ref. 11 and data not shown). Cell lines derived from each xenograft line (LX22CL, LX33CL, and LX36CL) also retained strong immunoreactivity for CD56 (data not shown).

To further characterize this model, we performed orthotopic tumor implantation using a transcutaneous injection approach. All three xenograft lines readily grew in the lungs of nude mice, where they formed discrete “primary tumors,” as well as metastasis to regional mediastinal lymph nodes (Fig. 1B), typical of the pattern seen in human SCLC patients. As shown in Fig. 1C, intrapulmonary tumors displayed typical SCLC histology and aggressively invaded lung parenchyma and vessels. These data show that this experimental system closely resembles human SCLC *in vivo*. An additional series of xenografts from well-characterized SCLC cell lines from ATCC were also generated, and all grew as flank xenografts with characteristic SCLC histology.

**Organization of gene expression analysis.** Samples of RNA derived from the primary xenograft model were grouped into “triplets” obtained from each primary xenograft (XG), its derived cell line (CL), and a secondary xenograft derived from that cell line (CLX). RNA was also purified from 11 well-characterized, commonly used SCLC cell lines (H69, H82, H128, H146, H187, H209, H345, H446, H526, H1618, and H1930) and their paired xenografts. *De novo* expression array analysis was then done on laboratory model triplets (XG, CL, and CLX) from three distinct patients (LX22, LX33, and LX36) on laboratory model pairs (CL and CLX) from ATCC SCLC cell lines and on total RNA from normal human lung and universal human reference RNA (Stratagene) using the hgu133plus2 Affymetrix array. These data were complemented with expression data from the public domain and with two *de novo* data sets, one accounting for four additional SCLC cell lines without a paired xenograft and one for four primary SCLC specimens independent from the laboratory models described above.

Public domain expression data were obtained from the GEO database (13), which included expression analyses of normal lung specimens, SCLC cell lines and xenografts, and primary tumors [series GSE3526, GSE7307, GSE8920, GSE7097 (29), GSE4127, GSE4824, GSE7670 (30), GSE2361, GSE6044 (31)], and one data set was obtained from the Broad Institute website<sup>10</sup> (32). Overall, 192 arrays from 13 data sets (five Affymetrix platforms) were analyzed, accounting for 62 normal lung samples, 19 primary SCLC, 4 primary xenografts (3 patients), 22 secondary xenografts, and 85 SCLC cell lines. Details of the samples and public domain

data used in this analysis are shown in Supplementary Table S1. Preprocessing details are reported in Supplementary Figs. S1 to S4.

**Differentially expressed genes in the primary xenograft model.** Results of the linear model analysis are shown in Fig. 2. The direct comparisons among the three different type of samples analyzed (XG, CL, and CLX) revealed three sets of differentially expressed genes: 395 were significantly different (adjusted  $P < 0.005$ ) when comparing primary xenografts (XG) to their matched derived cell line (CL), 152 were different when comparing XG to their derivative secondary xenografts (CLX), whereas only 26 genes were differentially expressed when comparing CL to CLX (Fig. 2A; Supplementary Tables A–C). Similar findings were obtained when the triplet samples were compared using gene expression changes with respect to the universal reference RNA or the normal lung specimen (Supplementary Figs. S5 and S6). The overall squared correlation among the groups of samples analyzed proved to be higher in all comparisons of derived cell lines with their derivative xenografts (Fig. 2B). Similarly, CAT plots show that a higher proportion of differentially expressed genes were in common between cell lines and their derivative xenografts (Fig. 2C; Supplementary Figs. S10 and S11). These data support the notion that gene expression programs change when cell lines are derived *in vitro*, and that the expression of a significant number of such genes is not restored when the derivative cell line is returned to growth *in vivo* as a xenograft.

**Analysis of functional annotation in the primary xenograft model.** Several functional themes were explored by analysis of functional annotation to discover common alterations in biological processes within the model. GO, KEGG, and functional gene sets from the MsigDb were used in a Wilcoxon rank-sum test after ordering the genes according to the moderated  $t$  statistics obtained after fitting the linear models. Overall, this analysis showed that both multiple pathways and biological processes are enriched in the comparisons between the model samples groups, and that different genes were responsible for the individual enrichments, including genes coding for transcription factors, adhesion and extracellular matrix molecules, apoptosis pathways, RNA metabolism, and metabolic enzymes. The results of this analysis using KEGG pathways are shown in Fig. 3. Highly significant enrichment was seen in several pathways relevant to preclinical cancer modeling, including keratan sulfate biosynthesis, the aminoacyl-tRNA biosynthesis pathway, mitogen-activated protein kinase signaling, transforming growth factor- $\beta$  signaling, apoptosis, and proteasomal function. The marked changes in gene expression in the apoptosis pathway are also consistent with the findings of Hann and colleagues (11), who showed that sensitivity to the BCL2 antagonist ABT-737 was a feature of SCLC cell lines and their paired xenografts and was associated with high-level BCL2 expression. Lower levels of BCL2 expression seen in our primary xenograft lines *in vivo* correlated with resistance to this therapy. All other results and the genes driving the enrichment are reported in Supplementary Figs. S13 to S16 and Supplementary Tables D and E.

**Analysis of changes in gene expression induced by cell culture.** To characterize gene expression changes induced by cell culture, we directly compared the model samples to primary tumors using linear model analysis in a combined data set accounting for primary SCLC specimens from several public sources and from our laboratory. We performed this analysis using all the genes in common among the platforms, before and after

<sup>10</sup> <http://www.broad.mit.edu/mpr/lung>

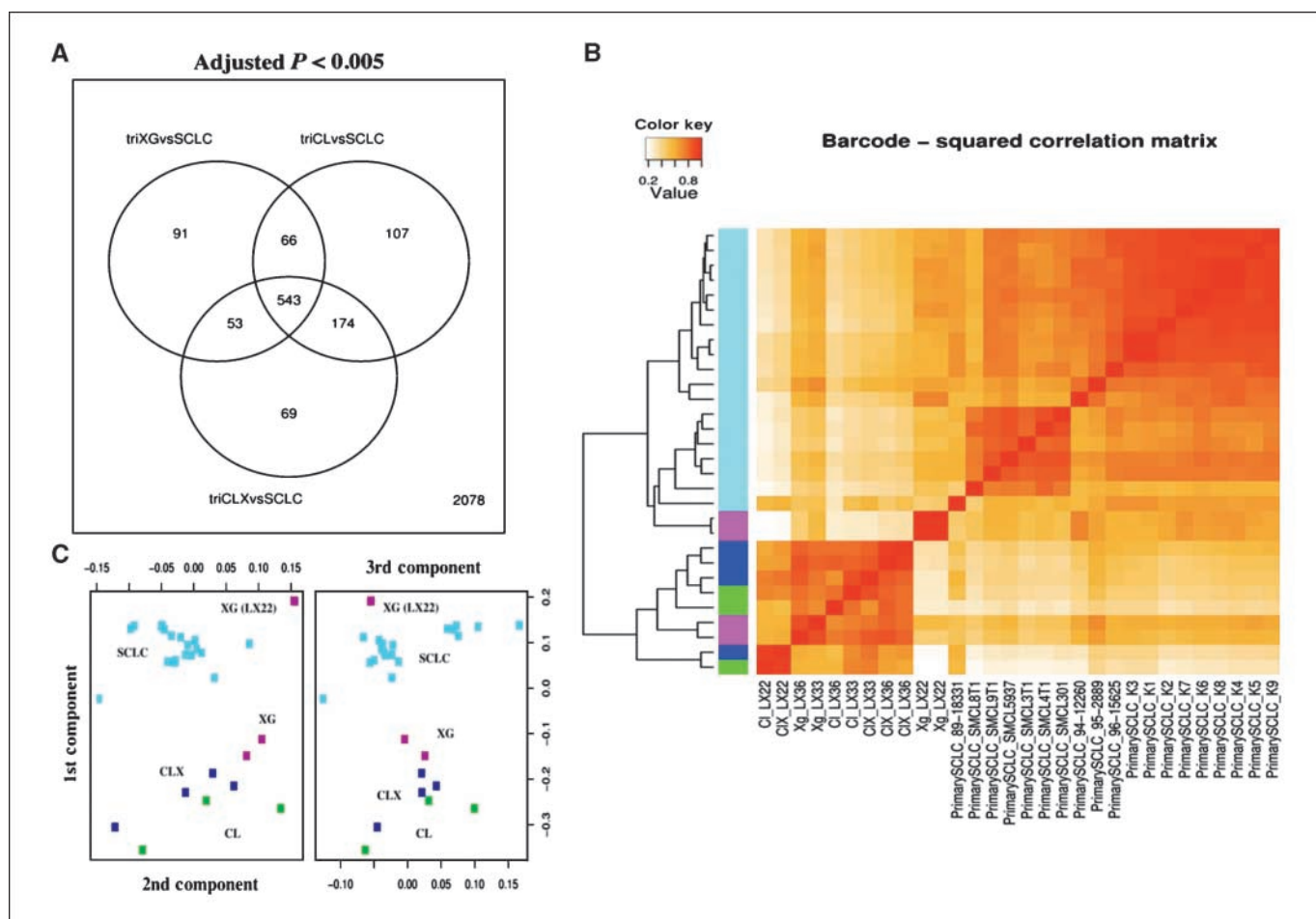


**Figure 4.** Comparison between laboratory model samples and primary SCLC specimens. **A**, Venn diagram showing the number of differentially expressed genes (adjusted  $P < 0.005$ ) in direct comparisons among primary xenografts (XG), the matched cell lines (CL), the xenografts obtained from these cell lines (CLX), and the group of primary SCLC. A group of 543 genes proved to be differentially expressed between all laboratory model groups (XG, CL, and CLX) and the primary SCLC. This group of genes accounts for genes expressed in cell types present only in primary tumors, such as genes expressed in lymphocytes and stromal cells present in the primary SCLC, and represents the difference in complexity between specimens obtained *in vivo* with respect to the laboratory models. A number of genes proved different between each group (XG, CL, and CLX) and the primary SCLC: Only 91 genes were differentially expressed between XG and SCLC, whereas 174 were genes differentially expressed between CL and CLX and SCLC. **B**, hierarchical clustering of all pairwise squared correlations between individual samples based on gene expression levels after barcode-RMA and quantile normalization. Individual primary SCLC (cyan), primary xenografts (XG; purple), cell lines (CL; green), and xenografts from these cell lines (CLX; blue) are shown. Correlations were computed using all genes (181) that proved to be differentially expressed (adjusted  $P < 0.05$ ) in any comparison between XG, CL, and CLX and that were present in all platforms. Overall, the primary xenografts (XG) proved to be more correlated with the primary SCLC than any other sample. Among primary xenografts (XG), the LX22 sample proved to be more correlated to primary SCLC than to its derivative CL and CLX. **C**, multidimensional scaling plot showing the relationships among all individual SCLC, XG, CL, and CLX samples. Cyan, SCLC; purple, XG; green, CL; blue, CLX. The XG samples from LX22 patient proved to be more similar to primary SCLC samples than were its derivative CL and CLX.

removing the interlaboratory effect using the empirical gene expression distribution described by Zilliox and Irizarry (ref. 16; see Supplementary Data). When we compared the models separately (XG, CL, or CLX) to the primary tumors, most of the differentially expressed genes were in common. This group of differentially expressed genes results from the comparison of fairly pure samples in terms of cell lineage (SCLC xenograft model samples) with a complex tissue accounting for stromal cells, lymphocytes, and cancer cells (the primary tumors). Nevertheless, a number of genes proved to change only in specific contrasts, and also in this case fewer differentially expressed genes were found when primary xenografts were compared with tumors than in the comparisons involving the cell lines and the secondary xenografts (Fig. 4A). In this aggregated analysis, we also compared the laboratory models and the primary SCLC to a large group of normal lung specimens, thus identifying the gene expression signature present in the

primary tumors and conserved in all the laboratory models (Supplementary Figs. S16 and S19–S25; Supplementary Table G).

One major problem when comparing expression array data from primary tumor samples with those derived from cell lines is that stromal and lymphoid gene expression in the primary tumor can create marked differences in gene expression that are not tumor specific. To overcome this problem, we searched for highly significant changes in gene expression within the three groups of the xenograft model (XG, CL, and CLX), where only human-specific, tumor-specific genes were analyzed. To this end, we selected genes whose expression varied in any comparison between our laboratory models (XG, CL, and CLX) and used this gene set to compare our xenograft model to primary SCLC samples. In this analysis, the primary xenografts more closely resembled primary tumors than did the derivative cell lines and secondary xenografts, as shown by all the pairwise squared correlations and by multidimensional

scaling of the first three components (Fig. 4B and C). This is particularly evident in the LX22 model, in which the differences in gene expression are evident in the primary xenograft but are lost both in the derivative cell line and secondary xenograft

(Fig. 4B and C). Similar findings were also obtained by using different stringency criteria to select the genes differentially expressed in the laboratory models and both by mapping the genes predicted in our direct comparison of the models

**Table 1.** List of genes that are permanently changed by cell culture

Entrez ID	Symbol	Gene name	Fold change (log 2)			Adjusted <i>P</i>		
			XGvsCL	CLvsCLX	XGvsCLX	XGvsCL	CLvsCLX	XGvsCLX
2261	<i>FGFR3</i>	fibroblast growth factor receptor 3	5.65	-0.4	5.25	0	0.91	0
94235	<i>GNG8</i>	guanine nucleotide binding protein (G protein), $\gamma 8$	4.94	-0.04	4.9	0	1	0
3306	<i>HSPA2</i>	heat shock 70kDa protein 2	4.84	-0.7	4.14	0.01	0.9	0.02
283120	<i>H19</i>	H19, imprinted maternally expressed transcript	4.96	-1.54	3.56	0	0.52	0.02
283131	<i>TncRNA</i>	trophoblast-derived noncoding RNA	4.11	-0.17	4.39	0	0.84	0
64065	<i>PERP</i>	PERP, TP53 apoptosis effector	4.43	-0.98	3.9	0.02	0.84	0.03
4821	<i>NKX2-2</i>	NK2 homeobox 2	4.17	-0.27	3.91	0.03	0.98	0.03
999	<i>CDH1</i>	cadherin 1, type 1, E-cadherin (epithelial)	4.09	-0.31	3.79	0.04	0.97	0.05
55466	<i>DNAJA4</i>	DnaJ (Hsp40) homologue, subfamily A, member 4	4.14	-0.31	3.74	0	0.25	0
4070	<i>TACSTD2</i>	tumor-associated calcium signal transducer 2	3.96	-0.22	3.67	0.01	0.4	0.02
7852	<i>CXCR4</i>	chemokine (C-X-C motif) receptor 4	4.22	-1.09	3.38	0	0.62	0.01
1299	<i>COL9A3</i>	collagen, type IX, $\alpha 3$	3.71	0.12	3.83	0	0.98	0
57007	<i>CXCR7</i>	chemokine (C-X-C motif) receptor 7	4.89	-0.25	2.64	0	0.53	0
6662	<i>SOX9</i>	SRY (sex determining region Y)-box 9	3.74	-0.29	3.54	0.03	0.97	0.03
54492	<i>LOC54492</i>	hypothetical LOC54492	3.82	-0.38	3.44	0.02	0.95	0.03
2820	<i>GPD2</i>	glycerol-3-phosphate dehydrogenase 2 (mitochondrial)	5.5	-0.5	1.75	0	0.92	0
164633	<i>CABP7</i>	calcium binding protein 7	3.47	0.17	3.64	0.02	0.98	0.02
219844	<i>HYLS1</i>	hydroletharus syndrome 1	3.66	-0.24	3.42	0.01	0.97	0.02
3481	<i>IGF2</i>	insulin-like growth factor 2 (somatomedin A)	2.54	-0.26	4.44	0.01	0.45	0.02
5349	<i>FXYD3</i>	FXYD domain containing ion transport regulator 3	3.58	-0.38	3.28	0.02	0.85	0.03
4246	<i>SCGB2A1</i>	secretoglobin, family 2A, member 1	3.55	-0.28	3.28	0.01	0.96	0.01
5617	<i>PRL</i>	prolactin	4.06	-1.32	2.74	0.01	0.59	0.04
3963	<i>LGALS7</i>	lectin, galactoside-binding, soluble, 7 (galectin 7)	3.23	0.28	3.51	0.05	0.97	0.03
25878	<i>MXRA5</i>	matrix-remodeling associated 5	3.3	0.05	3.35	0	0.99	0
10653	<i>SPINT2</i>	serine peptidase inhibitor, Kunitz type, 2	3.46	-0.36	3.1	0.03	0.96	0.04
2977	<i>GUCY1A2</i>	guanylate cyclase 1, soluble, $\alpha 2$	-2.07	0.26	-1.81	0.01	0.92	0.02
255231	<i>MCOLN2</i>	mucolipin 2	-1.6	-0.7	-2.31	0.03	0.72	0.02
8715	<i>NOLA4</i>	nucleolar protein 4	-2.19	0.39	-1.8	0.01	0.87	0.03
3709	<i>ITPR2</i>	inositol 1,4,5-triphosphate receptor, type 2	-1.87	-0.84	-2.11	0.01	0.53	0
11001	<i>SLC27A2</i>	solute carrier family 27 (fatty acid transporter), member 2	-1.84	-0.33	-2.17	0.04	0.91	0.02
54530	<i>C1orf218</i>	chromosome 1 open reading frame 218	-2.26	0.42	-1.84	0.01	0.87	0.04
6507	<i>SLC1A3</i>	(glial high affinity glutamate transporter), member 3	-1.89	-0.35	-2.25	0.03	0.62	0.01
5028	<i>P2RY1</i>	purinergic receptor P2Y, G-protein coupled, 1	-1.35	0.85	-2.8	0.05	0.44	0.02
7325	<i>UBE2E2</i>	ubiquitin-conjugating enzyme E2E 2	-2.25	-0.76	-1.91	0.02	0.51	0.03
169200	<i>TMEM64</i>	transmembrane protein 64	-2.22	-0.25	-2.03	0.01	0.38	0.04
5308	<i>PITX2</i>	paired-like homeodomain 2	-2.16	0.06	-2.1	0.02	0.99	0.03
51678	<i>MPP6</i>	membrane protein, palmitoylated 6	-2.18	-0.05	-2.22	0.02	0.99	0.02
1491	<i>CTH</i>	cystathionase (cystathionine $\gamma$ -lyase)	-2.54	1.24	-1.86	0	0.25	0.03
79071	<i>ELOVL6</i>	ELOVL family member 6	-2.54	0.49	-2.05	0.01	0.85	0.03
153	<i>ADRB1</i>	adrenergic, $\beta 1$ -, receptor	-2.34	0.14	-2.36	0.02	0.74	0.02
401097	<i>LOC401097</i>	Similar to LOC166075	-2.42	-0.29	-2.71	0.04	0.95	0.02
80144	<i>FRAS1</i>	Fraser syndrome 1	-2.33	-0.52	-2.82	0.03	0.57	0.01
594855	<i>CPLX3</i>	complexin 3	-2.89	1.08	-2.26	0.01	0.74	0.03
3049	<i>HBQ1</i>	hemoglobin, theta 1	-2.28	-0.6	-2.88	0.03	0.81	0.01
54941	<i>RNF125</i>	ring finger protein 125	-2.35	-0.47	-2.82	0.01	0.82	0
6096	<i>RORB</i>	retinoic acid receptor-related orphan receptor B	-2.65	0.8	-2.57	0.01	0.45	0.01
285368	<i>PRRT3</i>	proline-rich transmembrane protein 3	-2.91	0.54	-2.37	0.01	0.87	0.04
84864	<i>MINA</i>	MYC induced nuclear antigen	-2.69	0.55	-2.68	0.04	0.85	0.04
29953	<i>TRHDE</i>	thyrotropin-releasing hormone degrading enzyme	-3.05	0.4	-2.64	0	0.86	0
8835	<i>SOCS2</i>	suppressor of cytokine signaling 2	-3.82	1.16	-2.66	0	0.55	0.02

NOTE: The table shows the genes that are differentially expressed (adjusted *P* < 0.005) between XG and CL and between XG and CLX, but not between CL and CLX. Fold change (logarithmic scale on base 2) is shown for each comparison.

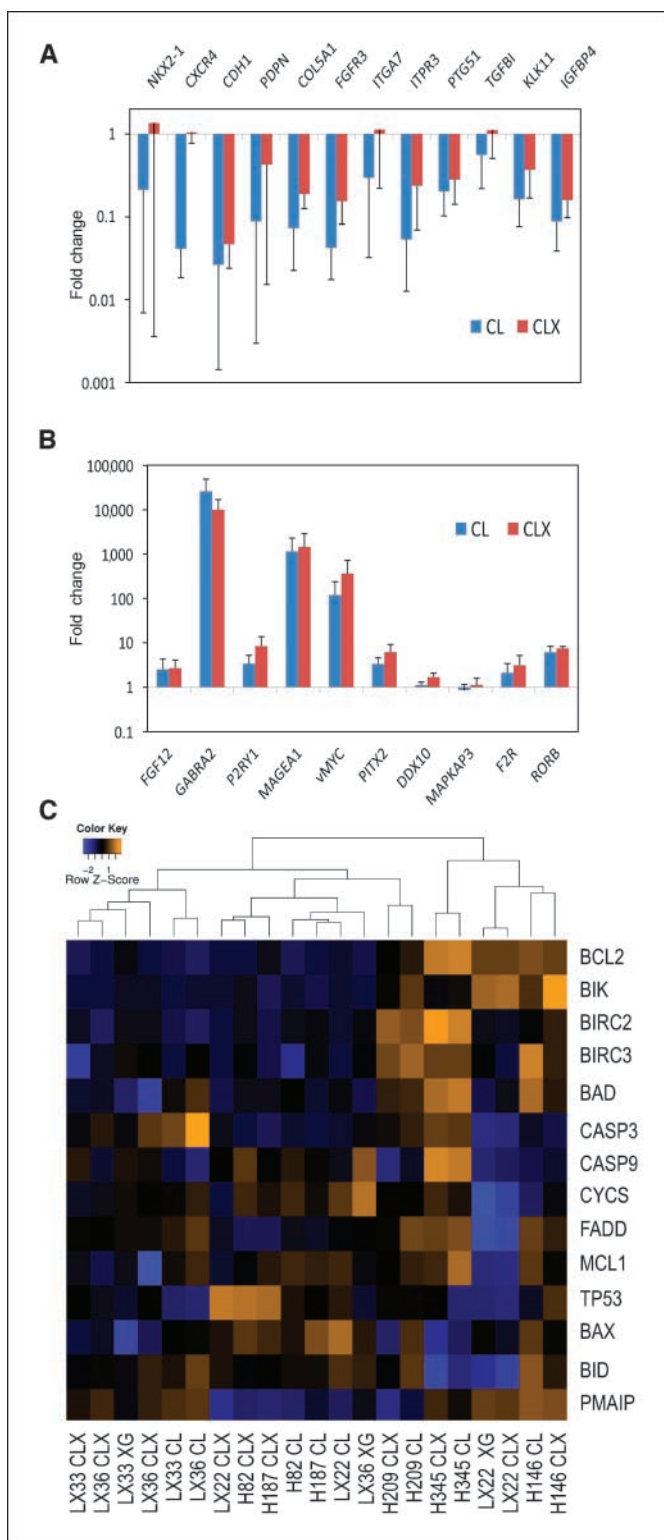


**Figure 5.** Validation of gene expression changes in the primary SCLC xenograft model. Expression levels in derivative cell lines (CL) and secondary xenografts (CLX) were compared with those in the corresponding primary xenograft, and are shown as the mean of paired data from all three xenograft lines ( $n = 6$ ); bars, SE. Genes selected from the microarray data (shown on the x axis) were up-regulated (A) or down-regulated (B) relative to expression in the primary xenograft samples. C, heat map expression analysis of BCL2-related genes in SCLC models. The RNA samples are listed as columns, and the genes in rows. The color scale represents the level of expression from low (blue) to high (orange).

(see Fig. 2) and by predicting the gene set on the combined data set (see Supplementary Data).

Most significantly, a group of genes was identified across the three models that were differentially expressed when comparing the primary xenograft lines, the xenograft-derived cell lines, and the secondary xenografts derived from these cell lines. This represents an expression signature of the permanent effects of tissue culture on gene expression in SCLC and includes genes known to be important in tumor growth, such as *IGFBP4*, *ITPR3*, *COX10*, *NKX2.1*, *CXCR4*, *CDH1*, *DAP3*, *CXCR7*, and *TLE2* (a detailed list of these genes is shown in Table 1 and Supplementary Table H).

Overall, these results show that tumor cells acclimated to standard cell culture conditions cannot completely regain the gene expression profile characteristic of SCLC in humans.

**Validation of gene expression changes.** We next sought to validate the gene expression changes observed in our primary xenograft model using quantitative real-time RT-PCR, with particular emphasis on expression changes that were not reversed when cell lines were reimplanted as xenografts. As shown in Fig. 5, irreversible changes in gene expression were quantitatively confirmed for 12 genes that were down-regulated (Fig. 5A) and 10 that were up-regulated (Fig. 5B) following the transition cell culture *in vitro*. These data confirm that marked changes in gene expression result during the transition from growth *in vivo* to culture *in vitro*, and that these changes are irreversible.

A recent study using our xenograft model analyzed the preclinical efficacy of the BCL2 antagonist ABT-737 as a potential targeted therapy for SCLC (11). Four cell lines (NCI-H146, H187, H209, and H345) proved sensitive, whereas the cell line H82, with markedly lower expression of BCL2 protein, proved resistant. The efficacy of ABT-737 in controlling the tumor growth *in vivo* using our primary xenografts models (LX22, LX33, and LX36) proved variable and seemed to correlate with BCL2 protein expression (11). As a further validation of our analysis, we determined the expression of *BCL2* and *BCL2*-related genes in the same models as those used in the ABT-737 study (11). As shown in the heat map analysis (Fig. 5C), the expression of *BCL2* and of functionally related genes such as *BID*, *BAX*, and *MCL1* varied significantly in the different SCLC models analyzed. In addition, the expression pattern of *BCL2* was consistent with the Western blot analysis of BCL2 protein expression in LX22, LX33, and LX36 (11). These data highlight the potential variability in preclinical cell culture models in the investigation of novel targeted agents.

## Discussion

Preclinical cancer biology and drug development have traditionally relied on the use of cell lines that are able to grow in serum-containing media and on artificial surfaces. Considerable debate has focused on the reliability of such cell lines as cancer models and of their ability to predict the success of novel therapies in humans (33–35). Recent attention has focused on the use of primary xenografts as a way to better model cancer *in vivo* (36). Although this approach is time-consuming and labor-intensive, there is emerging evidence that these models retain important biological properties that are seen in the primary tumor, including gene amplification (4), genomic architecture (37), characteristic histopathology (38–41), gene expression (42), and cancer stem cell biology (43, 44). By contrast, emerging evidence supports the contention that primary xenografts differ substantially from their

parent tumor by acquiring new genomic changes, faster growth rates, and nuclear pleomorphism (45, 46).

In 2007, Dangles-Marie and colleagues (47) compared colon cancer primary xenografts to matched cell lines, and showed variable changes in expression of a panel of 66 genes. Most importantly, these cell lines differed markedly in their sensitivities to standard chemotherapeutic agents derived from their matched xenografts (47). In our study, we explored the idea that primary xenografts may represent a useful preclinical model in SCLC, a tumor in which little therapeutic progress has been made in the last 30 years. Using a prospective, unbiased, bioinformatics-based approach, we were able to observe marked changes in gene expression as SCLC cells transitioned to standard cell culture conditions. In many cases, these changes were not reversed when cell lines were reestablished as xenografts. Even more striking was that these expression changes occurred in a large number of critically important cancer signaling pathways of direct relevance to targeted therapies, stromal interactions, developmental signaling, and chemosensitivity.

Interestingly, when analyzing the genes whose expression changed most significantly in the transition to cell culture, expression patterns in our primary xenograft lines were more closely matched to those seen in primary SCLC tissues than in cell lines or cell line-derived models. Moreover, the tendency of tissue

culture to reduce the differential gene expression patterns in lines derived from different patients suggests that heterogeneity in tumor cell biology may be underrepresented in cell culture systems. The ability of our SCLC models and of other primary xenograft systems to predict the therapeutic efficacy of cytotoxic and targeted agents in patients will be a more rigorous test of any potential clinical application of this approach.

## Disclosure of Potential Conflicts of Interest

C.D. Peacock received salary support through a gift from Genentech, Inc. D.N. Watkins is a former paid consultant for Genentech, Inc., with no ongoing financial interest. The other authors disclosed no potential conflicts of interest.

## Acknowledgments

Received 11/3/08; revised 2/10/09; accepted 2/13/09; published OnlineFirst 4/7/09.

**Grant support:** The American College of Surgeons (V.C. Daniel), NIH/National Cancer Institute Specialized Program of Research Excellence grant P50 CA058184 (D.N. Watkins, C.D. Peacock, W.L. Devereux, R. Yung), The Flight Attendant Medical Research Institute (D.N. Watkins, C.D. Peacock, C.M. Rudin, J.S. Hierman, and L. Marchionni), The Burroughs Wellcome Foundation (D.N. Watkins, C.M. Rudin), Genentech, Inc. (C.D. Peacock), and National Science Foundation grant DMS0342111 and NIH/National Cancer Research Foundation grant IU54RR023561-01A1 (L. Marchionni).

The costs of publication of this article were defrayed in part by the payment of page charges. This article must therefore be hereby marked *advertisement* in accordance with 18 U.S.C. Section 1734 solely to indicate this fact.

We thank Rafael Irizarry for comments and help with the analysis.

## References

- Jemal A, Siegel R, Ward E, Murray T, Xu J, Thun MJ. Cancer statistics, 2007. *CA Cancer J Clin* 2007;57:43–66.
- Pisick E, Jagadeesh S, Salgia R. Small cell lung cancer: from molecular biology to novel therapeutics. *J Exp Ther Oncol* 2003;3:305–18.
- Zochbauer-Muller S, Pirker R, Huber H. Treatment of small cell lung cancer patients. *Ann Oncol* 1999;10 Suppl 6:83–91.
- Pandita A, Aldape KD, Zadeh G, Guha A, James CD. Contrasting *in vivo* and *in vitro* fates of glioblastoma cell subpopulations with amplified EGFR. *Genes Chromosomes Cancer* 2004;39:29–36.
- De Witt Hamer PC, Van Tilborg AA, Eijk PP, et al. The genomic profile of human malignant glioma is altered early in primary cell culture and preserved in spheroids. *Oncogene* 2008;27:2091–6.
- Vescovi AL, Galli R, Reynolds BA. Brain tumour stem cells. *Nat Rev Cancer* 2006;6:425–36.
- Clement V, Sanchez P, de Tribolet N, Radovanovic I, Ruiz i Altaba A. HEDGEHOG-GLI1 signaling regulates human glioma growth, cancer stem cell self-renewal, and tumorigenicity. *Curr Biol* 2007;17:165–72.
- Sasai K, Romer JT, Lee Y, et al. Shh pathway activity is down-regulated in cultured medulloblastoma cells: implications for preclinical studies. *Cancer Res* 2006;66:4215–22.
- Phelps RM, Johnson BE, Ihde DC, et al. NCI-Navy Medical Oncology Branch cell line data base. *J Cell Biochem* 1996;24:32–91.
- Hodkinson PS, Mackinnon AC, Sethi T. Extracellular matrix regulation of drug resistance in small-cell lung cancer. *Int J Radiat Biol* 2007;83:733–41.
- Hann CL, Daniel VC, Sugar EA, et al. Therapeutic efficacy of ABT-737, a selective inhibitor of BCL-2, in small cell lung cancer. *Cancer Res* 2008;68:2321–8.
- Vertrees RA, Deyo DJ, Quast M, Lightfoot KM, Boor PJ, Zwischenberger JB. Development of a human to murine orthotopic xenotransplanted lung cancer model. *J Invest Surg* 2000;13:349–58.
- Wheeler DL, Barrett T, Benson DA, et al. Database resources of the National Center for Biotechnology Information. *Nucleic Acids Res* 2008;36:D13–21.
- Gentleman R, Carey VJ, Bates DM, et al. Bioconductor: open software development for computational biology and bioinformatics. *Genome Biol* 2004;R80:1465–6914.
- Irizarry RA, Hobbs B, Collin F, et al. Exploration, normalization, and summaries of high density oligonucleotide array probe level data. *Biostatistics* 2003;4:249–64.
- Zilliox MJ, Irizarry RA. A gene expression bar code for microarray data. *Nat Methods* 2007;4:911–3.
- Yang YH, Thorne N. Normalization for two color cDNA microarray data. *Science and Statistics: a Festschrift for Terry Speed*; 2003. p. 403–18.
- Ihaka R, Gentleman R. A language for data analysis and graphics. *J Comput Graph Stat* 1996;5:299–314.
- Smyth GK. Linear models and empirical Bayes methods for assessing differential expression in microarray experiments. *Stat Appl Genet Mol Biol* 2004;3:article3.
- Smyth GK, Michaud J, Scott HS. Use of within-array replicate spots for assessing differential expression in microarray experiments. *Bioinformatics* 2005;21:2067–75.
- Benjamini Y, Hochberg Y. Controlling the false discovery rate: a practical and powerful approach to multiple testing. *J R Stat Soc* 1995;57:289–300.
- Ashburner M, Ball CA, Blake JA, et al. The Gene Ontology Consortium. Gene ontology: tool for the unification of biology. *Nat Genet* 2000;25:25–9.
- Ashburner M, Lewis S. On ontologies for biologists: the Gene Ontology—untangling the web. *Novartis Found Symp* 2002;247:66–80; discussion 3, 4–90, 244–52.
- Harris MA, Clark J, Ireland A, et al. The Gene Ontology (GO) database and informatics resource. *Nucleic Acids Res* 2004;32:D258–61.
- Kanehisa M, Goto S, Kawashima S, Okuno Y, Hattori M. The KEGG resource for deciphering the genome. *Nucleic Acids Res* 2004;32:D277–80.
- Subramanian A, Tamayo P, Mootha VK, et al. Gene set enrichment analysis: a knowledge-based approach for interpreting genome-wide expression profiles. *Proc Natl Acad Sci U S A* 2005;102:15545–50.
- Mootha VK, Lepage P, Miller K, et al. Identification of a gene causing human cytochrome *c* oxidase deficiency by integrative genomics. *Proc Natl Acad Sci U S A* 2003;100:605–10.
- Irizarry RA, Warren D, Spencer F, et al. Multiple-laboratory comparison of microarray platforms. *Nat Methods* 2005;2:345–50.
- Olejniczak ET, Van Sant C, Anderson MG, et al. Integrative genomic analysis of small-cell lung carcinoma reveals correlates of sensitivity to bcl-2 antagonists and uncovers novel chromosomal gains. *Mol Cancer Res* 2007;5:331–9.
- Su LJ, Chang CW, Wu YC, et al. Selection of DDX5 as a novel internal control for Q-RT-PCR from microarray data using a block bootstrap re-sampling scheme. *BMC Genomics* 2007;8:140.
- Ge X, Yamamoto S, Tsutsumi S, et al. Interpreting expression profiles of cancers by genome-wide survey of breadth of expression in normal tissues. *Genomics* 2005;86:127–41.
- Bhattacharjee A, Richards WG, Staunton J, et al. Classification of human lung carcinomas by mRNA expression profiling reveals distinct adenocarcinoma subclasses. *Proc Natl Acad Sci U S A* 2001;98:13790–5.
- Johnson JI, Decker S, Zaharevitz D, et al. Relationships between drug activity in NCI preclinical *in vitro* and *in vivo* models and early clinical trials. *Br J Cancer* 2001;84:1424–31.
- Voskoglou-Nomikos T, Pater JL, Seymour L. Clinical predictive value of the *in vitro* cell line, human xenograft, and mouse allograft preclinical cancer models. *Clin Cancer Res* 2003;9:4227–39.
- Kerbel RS. Human tumor xenografts as predictive preclinical models for anticancer drug activity in humans: better than commonly perceived-but they can be improved. *Cancer Biol Ther* 2003;2: S134–9.
- Morton CL, Houghton PJ. Establishment of human tumor xenografts in immunodeficient mice. *Nat Protoc* 2007;2:247–50.
- Lefrançois D, Olschwang S, Delattre O, et al. Preservation of chromosome and DNA characteristics of human colorectal adenocarcinomas after passage in nude mice. *Int J Cancer* 1989;44:871–8.
- Lee CH, Xue H, Sutcliffe M, et al. Establishment of subrenal capsule xenografts of primary human ovarian

- tumors in SCID mice: potential models. *Gynecol Oncol* 2005;96:48–55.
39. Burg-Kurland CL, Purnell DM, Combs JW, Valerio MG, Harris CC, Trump BF. Immunocytochemical evaluation of primary human esophageal carcinomas and their xenografts for keratin,  $\beta$ -chorionic gonadotropin, placental lactogen,  $\alpha$ -fetoprotein, carcinoembryonic antigen, and nonspecific cross-reacting antigen. *Cancer Res* 1986;46:5730–7.
40. Alpaugh ML, Tomlinson JS, Shao ZM, Barsky SH. A novel human xenograft model of inflammatory breast cancer. *Cancer Res* 1999;59:5079–84.
41. Gray DR, Huss WJ, Yau JM, et al. Short-term human prostate primary xenografts: an *in vivo* model of human prostate cancer vasculature and angiogenesis. *Cancer Res* 2004;64:1712–21.
42. Rubio-Viqueira B, Jimeno A, Cusatis G, et al. An *in vivo* platform for translational drug development in pancreatic cancer. *Clin Cancer Res* 2006;12:4652–61.
43. Li C, Heidt DG, Dalerba P, et al. Identification of pancreatic cancer stem cells. *Cancer Res* 2007;67:1030–7.
44. Dalerba P, Dylla SJ, Park IK, et al. Phenotypic characterization of human colorectal cancer stem cells. *Proc Natl Acad Sci U S A* 2007;104:10158–63.
45. Beniers AJ, Peelen WP, Schaafsma HE, et al. Establishment and characterization of five new human renal tumor xenografts. *Am J Pathol* 1992;140:483–95.
46. Beniers AJ, van Moorselaar RJ, Peelen WP, Debruyne FM, Schalken JA. Differential sensitivity of renal cell carcinoma xenografts towards therapy with interferon- $\alpha$ , interferon- $\gamma$ , tumor necrosis factor and their combinations. *Urol Res* 1991;19:91–8.
47. Dangles-Marie V, Pocard M, Richon S, et al. Establishment of human colon cancer cell lines from fresh tumors versus xenografts: comparison of success rate and cell line features. *Cancer Res* 2007;67:398–407.